

---

# ROBUST LOCALIZATION IN WIRELESS NETWORKS FROM CORRUPTED SIGNALS

---

A PREPRINT

Muhammad Osama\*

Dave Zachariah\*

Satyam Dwivedi

Petre Stoica\*

## ABSTRACT

We address the problem of timing-based localization in wireless networks, when an unknown fraction of data is corrupted by nonideal propagation conditions. While timing-based techniques can enable accurate localization, they are sensitive to corrupted data. We develop a robust method that is applicable to a range of localization techniques, including time-of-arrival, time-difference-of-arrival and time-difference in schedule-based transmissions. The method is distribution-free and requires only an upper bound on the fraction of corrupted data, thus obviating distributional assumptions on the corrupting noise. The robustness of the method is demonstrated in numerical experiments.

## 1 Introduction

Localization in wireless networks is important for applications in GPS-denied environments [2]. The next generation wireless communication systems will standardize radio signals and measurements for localization in applications that range from mobile broadband to industrial internet-of-things networks. For accurate localization, these applications depend on techniques that use the signal time of flight between a transmitter and a receiver [1, 16].

Real-world measurements of wireless signals are prone to outliers which arise not only from sensor failures but also from signals that fail to reach the receiver in an ideal line-of-sight (LOS) manner. That is, wireless signals that may arrive at the receiver after reflections, diffractions or penetrations of different media, which we refer to as non-line-of-sight (NLOS) situations. The deployment of wireless technologies faces signal obstructions, moving objects, reflecting paths, foliage, etc. Under such non-ideal and NLOS conditions, standard measurement noise assumptions are invalid and conventional localization methods break down, as illustrated in Figure 1.

Several approaches to robust localization exist. A conservative approach is to model the NLOS effects as bounded additive measurement errors or bias [15, 17] and then estimate the node location that minimizes the worst-case error. This approach, however, can be overly conservative and sensitive to the user specified error bound. Another approach from the robust statistics literature is to consider the Huber contamination model [10], in which an  $\epsilon$  fraction of data samples are corrupted by a NLOS-data distribution. The NLOS distribution is either assumed to have a specific parametric form – e.g. shifted Gaussian or exponential [12, 19] in which case the positions of nodes are estimated via maximum likelihood – or is modelled nonparametrically [7, 8, 18], a case which is tackled using semiparametric or iterative maximum likelihood methods. An alternative approach is to use a different, robust loss function that is insensitive to outliers [21]. While it is often assumed that the fraction of corrupted data is known, in practice this fraction is an unknown user parameter.

In this paper, we propose a robust localization methodology for data obtained in the contamination setting with an unknown fraction  $\epsilon$  of NLOS data, drawing upon the principles of robust risk minimization in [13]. We only assume that the user is able to set an upper bound  $\tilde{\epsilon} \geq \epsilon$ . We demonstrate the methodology for three distinct localization techniques: time-of-arrival (TOA), time-difference-of-arrival (TDOA) and time-difference in schedule-based transmissions (TDST).

---

\*Division of System and Control, Department of Information Technology, Uppsala University, Sweden. muhammad.osama@it.uu.se, dave.zachariah@it.uu.se. This work was supported by the Swedish Research Council, Research Environment NewLEADS (contract 2016-06079) and projects (contracts 2017-04610 and 2018-05040).

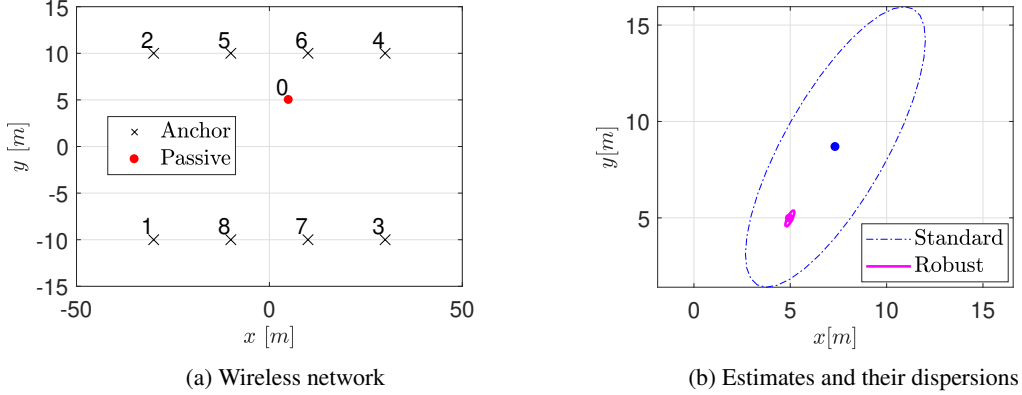


Figure 1: Self-localization of the passive receiving node (o) in (a) at location (5, 5) using eight anchor nodes (x) and time-difference of arrival (TDOA). The resolution of the interarrival times is on the order of 3ns and  $n = 100$  observations are used. Here  $\epsilon = 15\%$  of the data is corrupted by non-line of sight (NLOS) outliers. In (b), • and • denote the mean position estimated using the standard nonlinear least-squares method (8) and the proposed robust method. The ellipses illustrate the dispersion of location estimates with approximately 99.9% coverage for the standard (dotted) and robust (solid) methods.

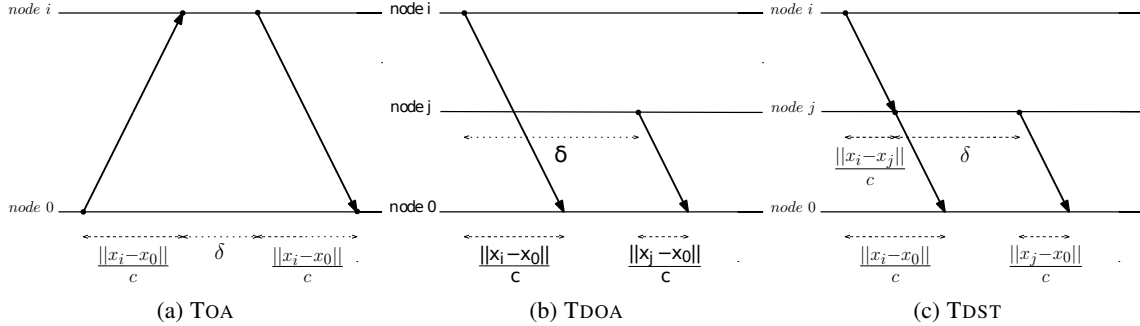


Figure 2: Timing diagrams illustrating node transmitting signals in three different localization techniques.

## 2 Problem formulation

For a general problem formulation, consider a wireless network consisting of  $N + 1$  nodes at locations

$$\{\mathbf{x}_0, \underbrace{\mathbf{x}_1, \dots, \mathbf{x}_{N_a}}_{\text{auxiliary}}, \underbrace{\mathbf{x}_{N_a+1}, \dots, \mathbf{x}_N}_{\text{anchors}}\}$$

in  $\mathbb{R}^d$  space, where  $d = 2$  or  $d = 3$ . Only the anchor node locations are known. The anchors and auxiliary nodes all transmit signals that propagate through space with constant velocity. These nodes can be thought of as base stations with known and unknown locations, respectively. The signals carry signatures that enable the identification of the transmitting node.

The self-localizing node, located at  $\mathbf{x}_0$ , can either be an active transceiver or a passive receiver, depending on the localization technique considered below. We let  $\theta^*$  denote the set of locations of interest and our goal is to estimate this set using timing measurements at node 0.

### 2.1 TOA: two-way ranging anchor nodes

In TOA, node  $\mathbf{x}_0$  is a transceiving node. At a given time, node 0 initiates a transmission to the anchor nodes. Upon receiving the signals, anchor nodes return signals, after a possible fixed delay. This leads to time-of-arrival measurements at self-localizing node 0. The TOA measurement with respect to anchor node  $i$  is then

$$\mu^{i0} = 2 \frac{\|\mathbf{x}_i - \mathbf{x}_0\|}{c} + \delta, \quad (1)$$

where  $c$  is the signal propagation velocity and  $\delta \geq 0$  is a transmission delay, see Figure 2a. The unknown location is

$$\boldsymbol{\theta}^* = \{\mathbf{x}_0\}$$

## 2.2 TDOA: synchronous anchor nodes

In TDOA, the anchor nodes are synchronized so that they broadcast signals with respect to a common clock. Consider a pair of anchor nodes  $(i, j)$  transmitting signals. Their interarrival time at the passive self-localizing receiver node 0 is then

$$\mu^{ij} = \frac{\|\mathbf{x}_j - \mathbf{x}_0\|}{c} + \delta - \frac{\|\mathbf{x}_i - \mathbf{x}_0\|}{c}, \quad (2)$$

where  $\delta \geq 0$  is a (possible) transmission delay at node  $i$ , see Figure 2b. The unknown location is

$$\boldsymbol{\theta}^* = \{\mathbf{x}_0\}$$

## 2.3 TDST: asynchronous anchor nodes

In TDST, the anchor nodes operate asynchronously so that the transmitted signals are only coordinated through a sequence of observable signal events. Consider a pair of transceiving nodes  $(i, j)$ , such that node  $j$  transmits only *after* receiving the signal from  $i$  and a given delay. The interarrival time at the passive node is then

$$\mu^{ij} = \frac{\|\mathbf{x}_i - \mathbf{x}_j\|}{c} + \frac{\|\mathbf{x}_j - \mathbf{x}_0\|}{c} + \delta - \frac{\|\mathbf{x}_i - \mathbf{x}_0\|}{c}. \quad (3)$$

where  $\delta > 0$  is the transmission delay at node  $j$ , see Figure 2c. As above, we consider

$$\boldsymbol{\theta}^* = \{\mathbf{x}_0, \}$$

However, we can readily accommodate unknown locations of auxiliary transmitting nodes in  $\boldsymbol{\theta}^*$  as demonstrated in the experimental section.

## 2.4 Measurements in LOS and NLOS

We let  $s \subseteq \{1, 2, \dots, N\}$  denote a set of transmitting nodes whose signals are observed by the self-localizing node. For a given  $s$ , the ideal interarrival times, from either (1), (2) or (3), can be arranged into a vector expressed as

$$\boldsymbol{\mu}(s, \boldsymbol{\theta}^*) = \frac{1}{c} \mathbf{M}(s) \boldsymbol{\rho}(\boldsymbol{\theta}^*) + \delta \mathbf{1}, \quad (4)$$

where

$$\boldsymbol{\rho}(\boldsymbol{\theta}^*) = \begin{bmatrix} \|\mathbf{x}_1 - \mathbf{x}_2\| \\ \|\mathbf{x}_1 - \mathbf{x}_3\| \\ \vdots \\ \|\mathbf{x}_1 - \mathbf{x}_N\| \\ \|\mathbf{x}_1 - \mathbf{x}_0\| \\ \vdots \\ \|\mathbf{x}_N - \mathbf{x}_0\| \end{bmatrix}$$

is an  $\frac{N(N+1)}{2} \times 1$  vector of distances between all nodes,  $\mathbf{M}(s)$  is a selection matrix of integers and  $\delta$  is a known delay parameter.

**Example 1 (TOA).** For  $N = 3$  and  $s = \{1, 2, 3\}$ , we have  $\boldsymbol{\mu}(s, \boldsymbol{\theta}^*) = [\mu^{10}, \mu^{20}, \mu^{30}]^\top$  and

$$\mathbf{M}(s) = \begin{bmatrix} 0 & 0 & 2 & 0 & 0 & 0 \\ 0 & 0 & 0 & 0 & 2 & 0 \\ 0 & 0 & 0 & 0 & 0 & 2 \end{bmatrix}$$

When  $s$  contains at least three anchor nodes that are not coaligned,  $\boldsymbol{\theta}^*$  is uniquely determined from the set of interarrival times, see [14].

**Example 2** (TDOA). For  $N = 3$  and  $s = \{1, 2, 3\}$ , we have  $\boldsymbol{\mu}(s, \boldsymbol{\theta}^*) = [\mu^{12}, \mu^{23}]^\top$  and

$$\mathbf{M}(s) = \begin{bmatrix} 0 & 0 & -1 & 0 & 1 & 0 \\ 0 & 0 & 0 & 0 & -1 & 1 \end{bmatrix}$$

in (4).

When  $s$  contains at least three anchor nodes that are not coaligned,  $\boldsymbol{\theta}^*$  is uniquely determined from the set of interarrival times, see [6].

**Example 3** (TDST). For  $N = 3$  and  $s = \{1, 2, 3, 1\}$ , we have  $\boldsymbol{\mu}(s, \boldsymbol{\theta}^*) = [\mu^{12}, \mu^{23}, \mu^{31}]^\top$  and

$$\mathbf{M}(s) = \begin{bmatrix} 1 & 0 & -1 & 0 & 1 & 0 \\ 0 & 0 & 0 & 1 & -1 & 1 \\ 0 & 1 & 1 & 0 & 0 & -1 \end{bmatrix}$$

in (4).

When  $s$  contains at least three anchor nodes that are not coaligned,  $\boldsymbol{\theta}^*$  can be uniquely determined from the set of interarrival times, see [20, sec. 3.3] and [3, 4].

In ideal LOS conditions, a set is drawn as  $s \sim p_{\text{LOS}}(s)$ , where the distribution is possibly degenerate. For each observed set  $s$ , the self-localizing node obtains noisy measurements  $\mathbf{z}$  of the interarrival times  $\boldsymbol{\mu}(s, \boldsymbol{\theta}^*)$ . That is,

$$\mathbf{z} \sim p_{\text{LOS}}(\mathbf{z}|s) \quad (5)$$

where the mean of  $p_{\text{LOS}}(\mathbf{z}|s)$  equals  $\boldsymbol{\mu}(s, \boldsymbol{\theta}^*)$  in (4).

In practical wireless environments, however, the pair  $(s, \mathbf{z})$  is not always observed in ideal conditions, but rather drawn from

$$p(s, \mathbf{z}) = (1 - \epsilon) p_{\text{LOS}}(s, \mathbf{z}) + \epsilon p_{\text{NLOS}}(s, \mathbf{z}), \quad (6)$$

where  $\epsilon$  is an unknown fraction of corrupted data and  $p_{\text{NLOS}}(s, \mathbf{z})$  is an unknown corrupting distribution, that generates outlier noise and biases such that its mean may differ from  $\boldsymbol{\mu}(s, \boldsymbol{\theta}^*)$  [10, 21]. The problem under consideration is to estimate  $\boldsymbol{\theta}^*$  given data  $\{(s_1, \mathbf{z}_1), \dots, (s_n, \mathbf{z}_n)\}$  drawn i.i.d. from (6). We merely assume that the quality of the data can be specified by an upper bound  $\tilde{\epsilon} \geq \epsilon$  [9, ch. 1].

### 3 Method

Assuming a set of anchor locations and transmission sequences that yield identifiable locations, we have that

$$\boldsymbol{\theta}^* \equiv \arg \min_{\boldsymbol{\theta}} \mathbb{E} \left[ \|\mathbf{z} - \boldsymbol{\mu}(s, \boldsymbol{\theta})\|^2 \right], \quad (7)$$

where the expectation is with respect to the unknown distribution  $p_{\text{LOS}}(s, \mathbf{z})$ . Note that the right-hand side of (7) assumes that  $\mathbf{z}$  has finite second-order moments. The standard estimator of  $\boldsymbol{\theta}^*$  is the nonlinear least-squares method,

$$\hat{\boldsymbol{\theta}} = \arg \min_{\boldsymbol{\theta}} \frac{1}{n} \sum_{i=1}^n \|\mathbf{z}_i - \boldsymbol{\mu}(s_i, \boldsymbol{\theta})\|^2, \quad (8)$$

where  $(s_i, \mathbf{z}_i) \sim p(s, \mathbf{z})$  in (6). Under standard regularity conditions  $\hat{\boldsymbol{\theta}}$  is consistent when  $\epsilon = 0$ , and corresponds to the maximum likelihood estimate assuming white Gaussian noise [11]. For  $\epsilon > 0$ , however,  $\hat{\boldsymbol{\theta}}$  is not robust to corrupted samples that arise in NLOS conditions, as described by (6).

#### 3.1 Robust localization

As an alternative to (7), consider the following fitting criterion

$$\mathbb{E}_{\boldsymbol{\pi}} \left[ \|\mathbf{z} - \boldsymbol{\mu}(s, \boldsymbol{\theta})\|^2 \right], \quad (9)$$

where, in lieu of  $p_{\text{LOS}}(s, \mathbf{z})$  in (7), we use the distribution

$$p(s, \mathbf{z}; \boldsymbol{\pi}) = \sum_{i=1}^n \pi_i \delta_{s_i, \mathbf{z}_i}(s, \mathbf{z}), \quad (10)$$

with probability weights  $\boldsymbol{\pi} = [\pi_1, \dots, \pi_n]^\top \in \Pi$ , where  $\Pi$  is the probability simplex. This distribution has an entropy

$$\mathbb{H}(\boldsymbol{\pi}) \triangleq - \sum_{i=1}^n \pi_i \ln \pi_i \geq 0 \quad (11)$$

It follows that the standard method (8) corresponds to minimizing (9) using the empirical distribution  $p(s, \mathbf{z}; n^{-1}\mathbf{1})$ , which attains a maximum entropy of  $\ln n$ .

Given the bound  $\tilde{\epsilon} \geq \epsilon$ , however, we expect at least  $(1 - \tilde{\epsilon})n$  uncorrupted samples and that the support of  $p(s, \mathbf{z}; \boldsymbol{\pi})$  should cover them. In this case, the maximum entropy would equal  $\ln[(1 - \tilde{\epsilon})n]$  and the search over the unknown support turns (9) into the following joint optimization problem

$$\begin{aligned} \min_{\boldsymbol{\theta}, \boldsymbol{\pi} \in \Pi} \quad & \sum_{i=1}^n \pi_i \|\mathbf{z}_i - \boldsymbol{\mu}(s_i, \boldsymbol{\theta})\|^2 \\ \text{subject to} \quad & \mathbb{H}(\boldsymbol{\pi}) \geq \ln[(1 - \tilde{\epsilon})n] \end{aligned} \quad (12)$$

Intuitively, the above minimization problem estimates  $\boldsymbol{\theta}$  and simultaneously assigns weights  $\pi_i$  to each point such that the overall weighted squared-error loss is minimized under the entropy constraint. Smaller weights are assigned to datapoints which are corrupted due to NLOS and larger weights are assigned to uncorrupted points. In this way, (12) enables robust localization of the auxiliary and receiver nodes without distributional assumptions. In the next subsection, we give a blockwise algorithm for solving (12).

### 3.2 Blockwise minimization algorithm

For a fixed  $\tilde{\boldsymbol{\theta}}$ , define

$$\hat{\boldsymbol{\pi}}(\tilde{\boldsymbol{\theta}}) = \begin{cases} \arg \min_{\boldsymbol{\pi} \in \Pi} \sum_{i=1}^n \pi_i \|\mathbf{z}_i - \boldsymbol{\mu}(s_i, \tilde{\boldsymbol{\theta}})\|^2, \\ \text{s.t. } \mathbb{H}(\boldsymbol{\pi}) \geq \ln[(1 - \tilde{\epsilon})n] \end{cases} \quad (13)$$

and, similarly, for a fixed  $\tilde{\boldsymbol{\pi}}$ , define

$$\hat{\boldsymbol{\theta}}(\tilde{\boldsymbol{\pi}}) = \arg \min_{\boldsymbol{\theta}} \sum_{i=1}^n \tilde{\pi}_i \|\mathbf{z}_i - \boldsymbol{\mu}(s_i, \boldsymbol{\theta})\|^2 \quad (14)$$

Together (13) and (14) form a blockwise coordinate descent algorithm which we summarize in Algorithm 1, that is guaranteed to converge to a critical point of (12) under fairly general conditions [5]. The weighted nonlinear least-squares problem in (14) can be solved using standard search methods (e.g. gradient-based or Newton search), while (13) requires solving a convex problem, whose solution can be obtained using a barrier method that is more efficient than general purpose numerical packages such as `cvx` [?].

---

#### Algorithm 1 Robust Localization

---

- 1: Input:  $\{(s_i, \mathbf{z}_i)\}_{i=1}^n$ ,  $\tilde{\epsilon}$  and  $\boldsymbol{\pi}^{(0)} = n^{-1}\mathbf{1}$
  - 2: Set  $k := 0$
  - 3: **repeat**
  - 4:  $\boldsymbol{\theta}^{(k+1)} = \hat{\boldsymbol{\theta}}(\boldsymbol{\pi}^{(k)})$
  - 5:  $\boldsymbol{\pi}^{(k+1)} = \hat{\boldsymbol{\pi}}(\boldsymbol{\theta}^{(k+1)})$
  - 6:  $k := k + 1$
  - 7: **until convergence**
  - 8: Output:  $\hat{\boldsymbol{\theta}} = \boldsymbol{\theta}^{(k)}$ ,  $\hat{\boldsymbol{\pi}} = \boldsymbol{\pi}^{(k)}$
- 

## 4 Experimental results

In this section, we illustrate the wide applicability of the proposed robust localization method using synthetic TOA, TDOA and TDST data. The performance is evaluated using the localization error

$$\Delta(\hat{\mathbf{x}}) = \|\mathbf{x} - \hat{\mathbf{x}}\|$$

where  $\mathbf{x}$  is the node location of interest.

We observe  $n = 100$  measurements from (6). The LOS distribution is

$$p_{\text{LOS}}(s, \mathbf{z}) = \underbrace{\mathcal{N}(\boldsymbol{\mu}(s, \boldsymbol{\theta}^*), \sigma_{\text{LOS}}^2 \mathbf{Q})}_{p_{\text{LOS}}(\mathbf{z}|s)} \underbrace{\mathcal{U}(s)}_{p_{\text{LOS}}(s)}, \quad (15)$$

where adjacent timing measurement errors have correlation structure given by  $\mathbf{Q}$ . The uniform distribution  $\mathcal{U}(s)$  draws  $s$  from a set  $\mathcal{S}$ . The corrupting NLOS distribution is

$$p_{\text{NLOS}}(s, \mathbf{z}) = \underbrace{\mathcal{E}(\boldsymbol{\mu}(s, \boldsymbol{\theta}^*) + \mu_{\text{NLOS}})}_{p_{\text{NLOS}}(\mathbf{z}|s)} \underbrace{\mathcal{U}(s)}_{p_{\text{NLOS}}(s)}, \quad (16)$$

where we consider an exponential distribution with measurement bias  $\mu_{\text{NLOS}}$ . We set  $\sigma_{\text{LOS}} = 3$  ns and  $\mu_{\text{NLOS}} = 75$  ns. Unless otherwise specified, the unknown corruption fraction is set to  $\epsilon = 15\%$ .

*Remark:* The code for the experiments is available at [github.com/Muhammad-Osama/RobustLocalization](https://github.com/Muhammad-Osama/RobustLocalization).

#### 4.1 TOA: two-way ranging anchor nodes

Consider a wireless network consisting of  $N = 8$  nodes as shown in Figure 1a. Since the TOA measurements are uncorrelated,  $\mathbf{Q} = \mathbf{I}$ . The unknown location of interest is

$$\boldsymbol{\theta}^* = \{\mathbf{x}_0\} = \{[5, 5]^\top\}.$$

The set  $\mathcal{S}$  consists of two sequences  $s_0 = \{6, 5, 7, 8\}$  and  $s_1 = \{4, 3, 2, 1\}$  where the node numbers are given in Figure 1a. The sequences have been selected so that the anchor nodes are not coaligned in either  $s_0$  or  $s_1$ .

In the case of TOA, the measurement model (1) admits an (overparameterized) linear form which is ideal for classical methods in robust statistics, such as the Huber method [21]. The Huber method is thus tailored for the task of TOA in which it provides a useful benchmark. We compare it to the standard nonlinear least-squares method (8) and the proposed method (12).

Figure 3a shows the cumulative distribution functions (CDF) of the localization error  $\Delta(\hat{\mathbf{x}})$  estimated from 100 Monte Carlo simulations, setting  $\tilde{\epsilon} = 20\%$  in Algorithm 1. As expected there is a severe performance degradation of the standard method. To investigate the sensitivity of the results to the unknown corruption fraction, we also plot the root-mean-square error (RMSE), i.e.  $\sqrt{\mathbb{E}[\Delta^2(\hat{\mathbf{x}})]}$ , versus  $\epsilon$  for all three methods. For the proposed method we set a very conservative upper bound  $\tilde{\epsilon} = 50\%$  in Algorithm 1. Figure 3b shows the RMSE for the different methods, where we see that the robust method is insensitive to  $\epsilon$ , with a graceful rise in RMSE when  $\epsilon$  exceeds  $\tilde{\epsilon}$ . In sum, the proposed method outperforms the standard nonlinear least-squares method and is close to the benchmark provided by the TOA-tailored Huber method.

The results are corroborated also in Figure 4 which shows RMSE as a function of  $\mathbf{x}_0$ . It can be seen that the robust method is more sensitive than the benchmark only near the edges of the vertical boundaries, where the

resolution of time-differences decreases.

#### 4.2 TDOA: synchronous anchor nodes

We consider again the network in Figure 1a, but now the self-localizing node is a passive receiver. Since TDOA measurements are correlated, we set  $\mathbf{Q}$  with 1s along the diagonal and  $1/3$  along the off-diagonals. The unknown location of interest is

$$\boldsymbol{\theta}^* = \{\mathbf{x}_0\} = \{[5, 5]^\top\}.$$

As in the case of TOA above, we use the sequence set  $\mathcal{S}$  with  $s_0 = \{6, 5, 7, 8\}$  and  $s_1 = \{4, 3, 2, 1\}$ .

Note that the measurement model (2) is nonlinear in  $\boldsymbol{\theta}$  and does not admit a linear re-parametrization. Thus the Huber method is not readily applicable for TDOA as it requires tuning an alternative numerical search techniques. We therefore compare only the standard nonlinear least-squares method (8) and the proposed method (12).

Figure 5a shows CDFs of the localization error  $\Delta(\hat{\mathbf{x}})$  estimated using 100 Monte Carlo simulations, setting  $\tilde{\epsilon} = 20\%$  in Algorithm 1. The performance characteristics are similar to those in Figure 3a, but the absolute error levels are not directly comparable due to different measurement setups. The sensitivity to the unknown corruption fraction  $\epsilon$  is also shown in Fig. 5b when RMSE is plotted against  $\epsilon$  for both methods. We use a very conservative upper bound  $\tilde{\epsilon} = 50\%$  in Algorithm 1. The proposed method is consistently robust and insensitive to corrupted data in contrast to

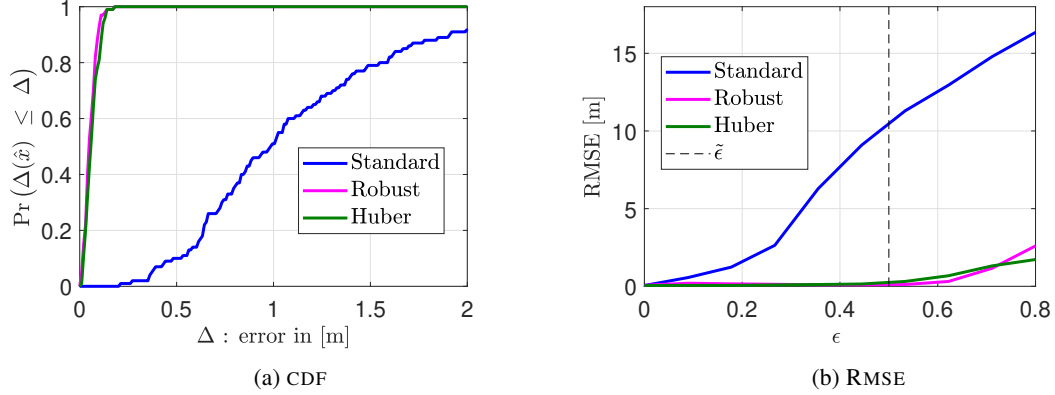


Figure 3: Performance and sensitivity in TOA. (a) Cumulative distribution functions of localization errors  $\Delta(\hat{x})$  of target node in Figure 1a using 100 Monte Carlo runs. Unknown corruption fraction was  $\epsilon = 15\%$  and the upper bound used in the robust method was set to  $\tilde{\epsilon} = 20\%$ . (b) Root-mean square error in [m] as a function of  $\epsilon$  for the target node using standard, robust and Huber methods. Results based on 50 Monte Carlo simulations. For the proposed robust method the upper bound was  $\tilde{\epsilon} = 50\%$ .

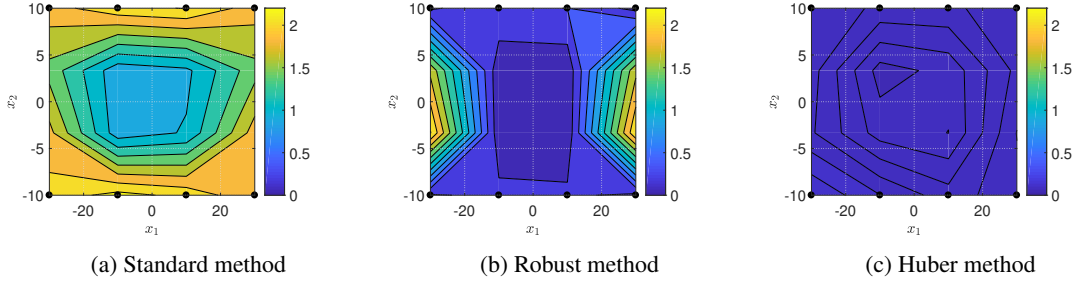


Figure 4: Performance in TOA across space. Root-mean square error in [m] with respect to different locations  $x_0$ . Results based on 50 Monte Carlo runs.

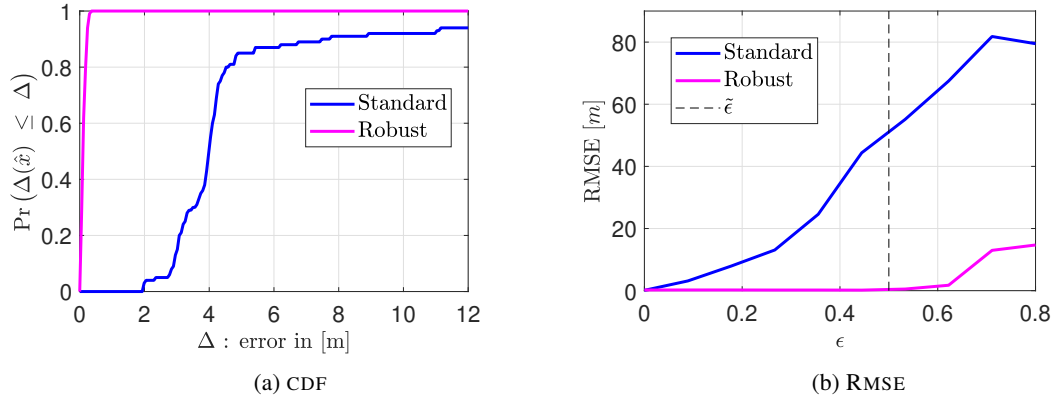


Figure 5: Performance and sensitivity in TDOA. (a) Cumulative distribution functions of localization errors  $\Delta(\hat{x})$  of target node in Figure 1a using 100 Monte Carlo runs. Unknown corruption fraction was  $\epsilon = 15\%$  and the upper bound used in the robust method was set to  $\tilde{\epsilon} = 20\%$ . (b) Root-mean square error in [m] as a function of  $\epsilon$  for the target node using standard and robust methods. Results based on 50 Monte Carlo simulations. For the proposed robust method the upper bound was  $\tilde{\epsilon} = 50\%$ .

the standard method for which the errors rise drastically with  $\epsilon$ . Figure 6 shows that the robust method yields substantial error reduction across space.

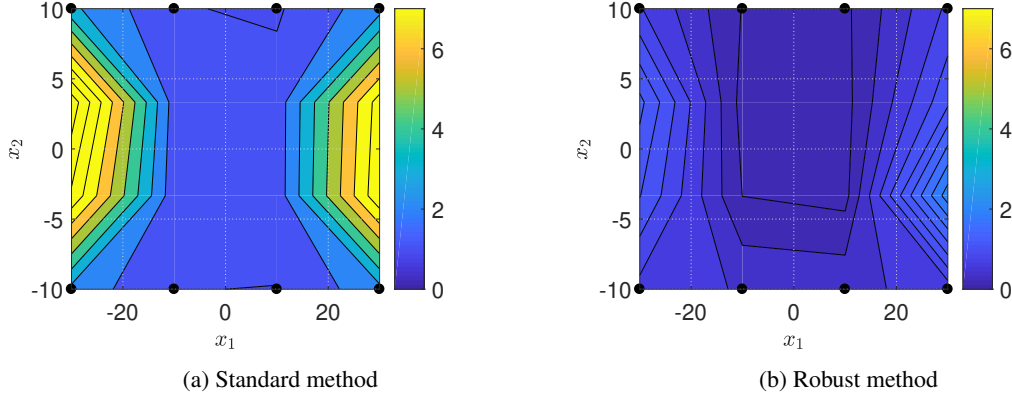


Figure 6: Performance in TDOA across space. Root-mean square error in [m] with respect to different locations  $\mathbf{x}_0$ . Results based on 50 Monte Carlo runs.

Finally, we illustrate the ability of the proposed method to effectively isolate corrupted NLOS samples. Since the data is generated synthetically we can classify each sample from  $p_{\text{NLOS}}(\mathbf{z}|s)$  as  $\mathcal{C}(\mathbf{z}) = 1$  for ‘corrupted’ or  $\mathcal{C}(\mathbf{z}) = 0$  for ‘normal’. The method solves (12) and learns the probability weights  $\hat{\pi}$ . If a weight is below a certain threshold, we may classify the corresponding sample  $\mathbf{z}$  as an outlier, i.e.,  $\hat{\mathcal{C}}(\mathbf{z}) = 1$ . We set the weight threshold to  $10^{-5}$  and show the resulting probability of correct detection  $\Pr\{\hat{\mathcal{C}}(\mathbf{z}) = 1 | \mathcal{C}(\mathbf{z}) = 1\}$  as well as the probability of false alarm  $\Pr\{\hat{\mathcal{C}}(\mathbf{z}) = 1 | \mathcal{C}(\mathbf{z}) = 0\}$  in Figure 7. We use  $\tilde{\epsilon} = 50\%$  and vary the unknown fraction  $\epsilon$ , using 50 Monte Carlo runs for each value of  $\epsilon$ . It can be seen that the proposed method can effectively isolate NLOS samples with a low false-alarm rate.

### 4.3 TDST: asynchronous anchor nodes

We consider the network in Figure 1a, but now the self-localizing node is a passive receiver and the anchor nodes are asynchronous. Since TDST measurements are correlated, we set  $\mathbf{Q}$  with 1s along the diagonal and  $1/3$  along the off-diagonals. The unknown location of interest is

$$\boldsymbol{\theta}^* = \{\mathbf{x}_0\} = \{[5, 5]^\top\}.$$

We use a set  $\mathcal{S}$  that consists of four sequences:  $s_0 = \{6, 4, 5, 3\}$ ,  $s_1 = \{3, 6, 4, 5\}$ ,  $s_2 = \{5, 3, 6, 4\}$  and  $s_3 = \{4, 5, 3, 6\}$ , following the scheme described in [4].

Similar to TDOA, the Huber method is not readily applicable to TDST. We therefore compare only the standard nonlinear least-squares method (8) and the proposed method (12).

Figure 8a shows the CDFs of the localization error  $\Delta(\hat{\mathbf{x}})$ . The characteristics are similar to those in Figure 3a. The sensitivity to the unknown corruption fraction  $\epsilon$  is shown in Fig. 8b where RMSE is plotted versus  $\epsilon$  for a very conservative upper bound  $\tilde{\epsilon} = 50\%$  in Algorithm 1. It can be seen that the proposed method also robustifies self-localization in TDST.

Finally, we consider a more challenging wireless network configuration, where one anchor node is replaced by an auxiliary node ( $N_a = 1$ ) at an unknown location as shown in Figure 9a. The goal is to passively localize auxiliary nodes using asynchronous anchor nodes [3, 4, 20] in adverse NLOS conditions. The locations of interest are

$$\boldsymbol{\theta}^* = \{\mathbf{x}_0, \mathbf{x}_1\} = \{[5, 5]^\top, [-10, 10]^\top\}.$$

We use a set  $\mathcal{S} = \{s_0, s_1\}$ , where  $s_0 = \{2, 3, 4, 5, 6, 7, 8, 2, 3, 4, 5, 6, 7, 8\}$  and  $s_1 = \{2, 1, 3, 1, 4, 1, 5, 1, 6, 1, 7, 1, 8, 1\}$ . The first sequence set  $s_0$  involves only the anchor nodes and ensures that the passive node location is identifiable. The second sequence  $s_1$  ensures that the auxiliary node location is identifiable, see [20].

Figure 9b summarizes the distribution of localization errors  $\Delta(\hat{\mathbf{x}})$  for the passive and auxiliary nodes. Note that this is a harder problem that involves two unknown locations  $\mathbf{x}_0$  and  $\mathbf{x}_1$ . Moreover, when estimating  $\mathbf{x}_1$  the difficulty is compounded. In Figure 9c we see that the localization

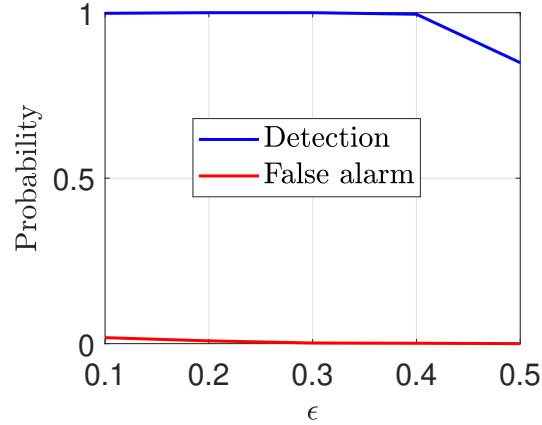


Figure 7: The weights in the robust method can be used to classify samples  $\mathcal{C}(z) \in \{0, 1\}$  as ‘normal’ or ‘corrupted’. This yields probabilities of correct detection  $\Pr\{\hat{\mathcal{C}}(z) = 1 | \mathcal{C}(z) = 1\}$  and false alarm  $\Pr\{\hat{\mathcal{C}}(z) = 1 | \mathcal{C}(z) = 0\}$  shown in the figure as the corruption fraction  $\epsilon$  is varied from 10% to 50%  $= \tilde{\epsilon}$ .

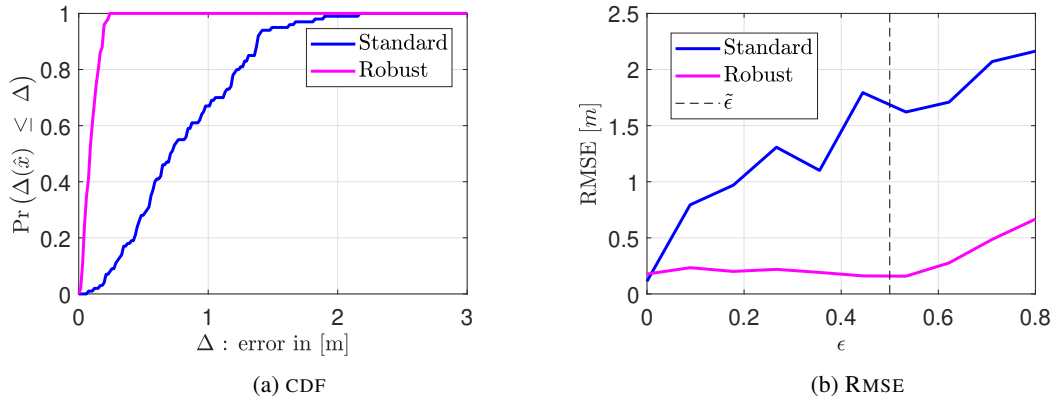


Figure 8: Performance and sensitivity in TDST. (a) Cumulative distribution functions of localization errors  $\Delta(\hat{x})$  of target node in Figure 1a using 100 Monte Carlo runs. Unknown corruption fraction was  $\epsilon = 15\%$  and the upper bound used in the robust method was set to  $\tilde{\epsilon} = 20\%$ . (b) Root-mean square error in [m] as a function of  $\epsilon$  for the target node using standard and robust methods. Results based on 50 Monte Carlo simulations. For the proposed robust method the upper bound was  $\tilde{\epsilon} = 50\%$ .

performance degrades rapidly under NLOS conditions using the standard method, whereas the proposed method is resilient.

## 5 Conclusion

We have developed a robust method for localization of nodes in wireless networks using timing-based measurements. The method is applicable to a wide range of localization technologies. Its robustness properties against data corrupted due to non-ideal and non-line-of-sight signal conditions are demonstrated using three different configurations: TOA, TDOA and TDST. The proposed method does not make any assumptions on the form of corrupting noise distribution, and only requires an upper bound on the fraction of corrupted data.

## References

- [1] Amir Beck, Petre Stoica, and Jian Li. Exact and approximate solutions of source localization problems. *IEEE Transactions on signal processing*, 56(5):1770–1778, 2008.

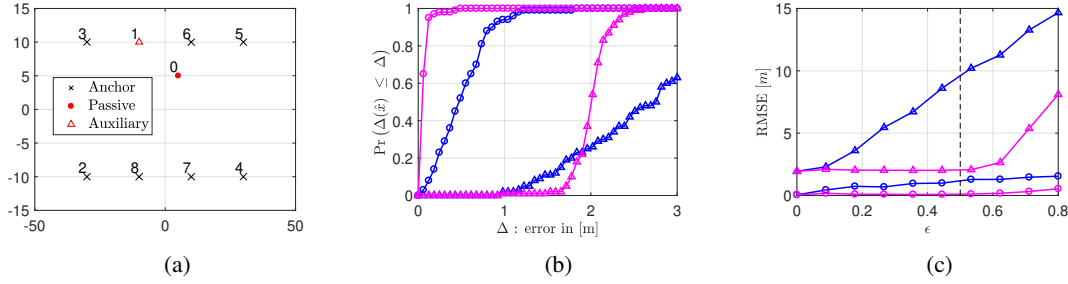


Figure 9: Performance and sensitivity in TDST when localizing additional auxiliary node. (a) Configuration of wireless network. (b) CDF of localization errors  $\Delta(\hat{\mathbf{x}})$  using 100 Monte Carlo runs for auxiliary (triangle) and passive node (circle), using the standard (blue) and robust (magenta) methods, respectively. Unknown corruption fraction is  $\epsilon = 15\%$  and  $\tilde{\epsilon} = 20\%$ . (c) Root mean square error as a function of the fraction of corrupted data  $\epsilon$  using standard (blue) and robust (magenta) method, for passive (circles) and auxiliary (triangles) nodes, respectively. Results based on 50 Monte Carlo simulations.  $\tilde{\epsilon} = 50\%$  indicated by the black-dashed line.

- [2] James J Caffery and Gordon L Stuber. Overview of radiolocation in cdma cellular systems. *IEEE Communications Magazine*, 36(4):38–45, 1998.
- [3] Baptiste Cavarec, Satyam Dwivedi, Mats Bengtsson, and Peter Händel. Schedule based self localization of asynchronous wireless nodes with experimental validation. In *2017 IEEE International Conference on Acoustics, Speech and Signal Processing (ICASSP)*, pages 5975–5979. IEEE, 2017.
- [4] Satyam Dwivedi, Alessio De Angelis, and Peter Händel. Scheduled uwb pulse transmissions for cooperative localization. In *2012 IEEE International Conference on Ultra-Wideband*, pages 6–10. IEEE, 2012.
- [5] Luigi Grippo and Marco Sciandrone. On the convergence of the block nonlinear gauss–seidel method under convex constraints. *Operations research letters*, 26(3):127–136, 2000.
- [6] Fredrik Gustafsson and Fredrik Gunnarsson. Positioning using time-difference of arrival measurements. In *2003 IEEE International Conference on Acoustics, Speech, and Signal Processing, 2003. Proceedings.(ICASSP'03).*, volume 6, pages VI–553. IEEE, 2003.
- [7] Ulrich Hammes, Eric Wolsztynski, and Abdelhak M Zoubir. Semi-parametric geolocation estimation in nlos environments. In *2008 16th European Signal Processing Conference*, pages 1–5. IEEE, 2008.
- [8] Ulrich Hammes, Eric Wolsztynski, and Abdelhak M Zoubir. Robust tracking and geolocation for wireless networks in nlos environments. *IEEE Journal of Selected Topics in Signal Processing*, 3(5):889–901, 2009.
- [9] Frank R Hampel, Elvezio M Ronchetti, Peter J Rousseeuw, and Werner A Stahel. *Robust statistics: the approach based on influence functions*, volume 196. John Wiley & Sons, 2011.
- [10] Peter J Huber. *Robust statistics*. Springer, 2011.
- [11] S.M. Kay. *Fundamentals of Statistical Signal Processing, Vol.1—Estimation theory*. Prentice Hall, 1993.
- [12] Michael McGuire, Konstantinos N Plataniotis, and Anastasios N Venetsanopoulos. Data fusion of power and time measurements for mobile terminal location. *IEEE Transactions on Mobile Computing*, 4(2):142–153, 2005.
- [13] Muhammad Osama, Dave Zachariah, and Peter Stoica. Robust risk minimization for statistical learning. *IEEE Open Journal of Signal Processing*, 2020.
- [14] S Ravindra and SN Jagadeesha. Time of arrival based localization in wireless sensor networks: A linear approach. *arXiv preprint arXiv:1403.6697*, 2014.
- [15] Xiufang Shi, Brian DO Anderson, Guoqiang Mao, Zaiyue Yang, Jiming Chen, and Zihuai Lin. Robust localization using time difference of arrivals. *IEEE Signal Processing Letters*, 23(10):1320–1324, 2016.
- [16] Petre Stoica and Jian Li. Lecture notes–source localization from range-difference measurements. *IEEE Signal Processing Magazine*, 23(6):63–66, 2006.
- [17] Slavisa Tomic, Marko Beko, Rui Dinis, and Paulo Montezuma. A robust bisection-based estimator for toa-based target localization in nlos environments. *IEEE Communications Letters*, 21(11):2488–2491, 2017.
- [18] Feng Yin, Carsten Fritsche, Fredrik Gustafsson, and Abdelhak M Zoubir. Toa-based robust wireless geolocation and cramér-rao lower bound analysis in harsh los/nlos environments. *IEEE transactions on signal processing*, 61(9):2243–2255, 2013.

- 
- [19] Feng Yin, Abdelhak M Zoubir, Carsten Fritsche, and Fredrik Gustafsson. Robust cooperative sensor network localization via the em criterion in los/nlos environments. In *2013 IEEE 14th Workshop on Signal Processing Advances in Wireless Communications (SPAWC)*, pages 505–509. IEEE, 2013.
  - [20] Dave Zachariah, Alessio De Angelis, Satyam Dwivedi, and Peter Händel. Schedule-based sequential localization in asynchronous wireless networks. *EURASIP Journal on Advances in Signal Processing*, 2014(1):16, 2014.
  - [21] Abdelhak M Zoubir, Visa Koivunen, Esa Ollila, and Michael Muma. *Robust statistics for signal processing*. Cambridge University Press, 2018.